

Maximization of Fundamental Frequencies of Axially Compressed Laminated Curved Panels against Fiber Orientation

Hsuan-Teh Hu¹ and Jun-Ming Chen²

Abstract: Free vibration analyses of laminated curved panels subjected to axial compressive forces are carried out by employing the Abaqus finite element program. The fundamental frequencies of these composite laminated curved panels with a given material system are then maximized with respect to fiber orientations by using the golden section method. Through a parametric study, the significant influences of the end conditions, the panel aspect ratio, the panel curvature and the compressive force on the maximum fundamental frequencies and the associated optimal fiber orientations are demonstrated and discussed.

Keywords: Maximization, fundamental frequencies, axially compressed laminated curved panels.

1 Introduction

The applications of fiber-composite laminate materials to aerospace industrial such as spacecraft, high-speed aircraft and satellite have increased rapidly in recent years. The most major components of the aerospace structures are frequently made of curved panels and subjected to various kinds of compressive forces. Therefore, knowledge of the dynamic characteristics of composite laminated curved panels in compression, such as their fundamental natural frequency, is essential.

The fundamental natural frequency of composite laminated curved panels highly depends on the ply orientations (Crawley, 1979; Chandrashekhara, 1989; Qatu and Leissa, 1991; Raouf, 1994; Chun and Lam, 1995; Hu and Juang, 1997; Hu and Tsai, 1999; Hu and Ou, 2001; Hu and Tsai, 2009), end conditions (Sharma and Darvizeh, 1987; Chandrashekhara, 1989; Chun and Lam, 1995; Hu and Juang, 1997; Hu and Tsai, 1999), geometries (Chandrashekhara, 1989; Qatu and Leissa, 1991; Hu

¹ Department of Civil Engineering and Sustainable Environment Research Center, National Cheng Kung University, Tainan, Taiwan 701, R.O.C.

² Department of Civil Engineering, National Cheng Kung University, Tainan, Taiwan 701, R.O.C.

and Juang, 1997; Hu and Tsai, 1999; Hu and Ou, 2001; Hu and Tsai, 2009), and compressive forces (Dhanaraj and Palanininathan, 1990; Chen, Cheng, Chien and Doong, 2002; Nayak, Moy and Shenoi, 2005; Chakrabarti, Topdar and Sheikh, 2006; Hu and Tsai, 2009). Therefore, proper selection of appropriate lamination to maximize the fundamental frequency of composite laminated curved panels in compression becomes a crucial problem (Bert, 1991; Abrate, 1994; Raouf, 1994; Topal and Uzman, 2006).

Research on the subject of structural optimization has been reported by many investigators (Schmit, 1981) and has been widely employed to study the dynamic behavior of composite structures (Abate, 1994; Hu, and Ho, 1996; Hu and Juang, 1997; Hu and Tsai, 1999; Hu and Ou, 2001; Narita, 2003; Topal and Uzman, 2006; Hu and Wang, 2007; Hu and Tsai, 2009). Among various optimization schemes, the golden section method is a simple technique and can be easily programmed for solution on the computer (Vanderplaats, 1984; Haftka, Gürdal and Kamat, 1990). In this investigation, maximization of the fundamental natural frequency of composite laminated curved panels in compression with respect to fiber orientations is performed by using the golden section method. The fundamental frequencies of composite laminated curved panels are calculated by using the Abaqus finite element program (Abaqus, Inc., 2010). In the paper, the constitutive equations for fiber-composite lamina, vibration analysis and golden section method are briefly reviewed. The influences of the end conditions, the panel aspect ratio, the panel curvature and the compressive force on the maximum fundamental natural frequency and the associated optimal fiber orientations of the laminated curved panels are presented and important conclusions obtained from the study are given.

2 Constitutive matrix for fiber-composite laminae

In the finite element analysis, the laminated cylindrical shells are modeled by eight-node isoparametric shell elements with six degrees of freedom per node (three displacements and three rotations). The reduced integration rule together with hourglass stiffness control is employed to formulate the element stiffness matrix (Abaqus, Inc., 2010).

During the analysis, the constitutive matrices of composite materials at element integration points must be calculated before the stiffness matrices are assembled from element level to global level. For fiber-composite laminate materials, each lamina can be considered as an orthotropic layer. The stress-strain relations for a lamina in the material coordinate (1,2,3) (Fig. 1) at an element integration point can be written as

$$\{\sigma'\} = [Q_1']\{\varepsilon'\}, \quad \{\tau'\} = [Q_2']\{\gamma'\} \quad (1)$$

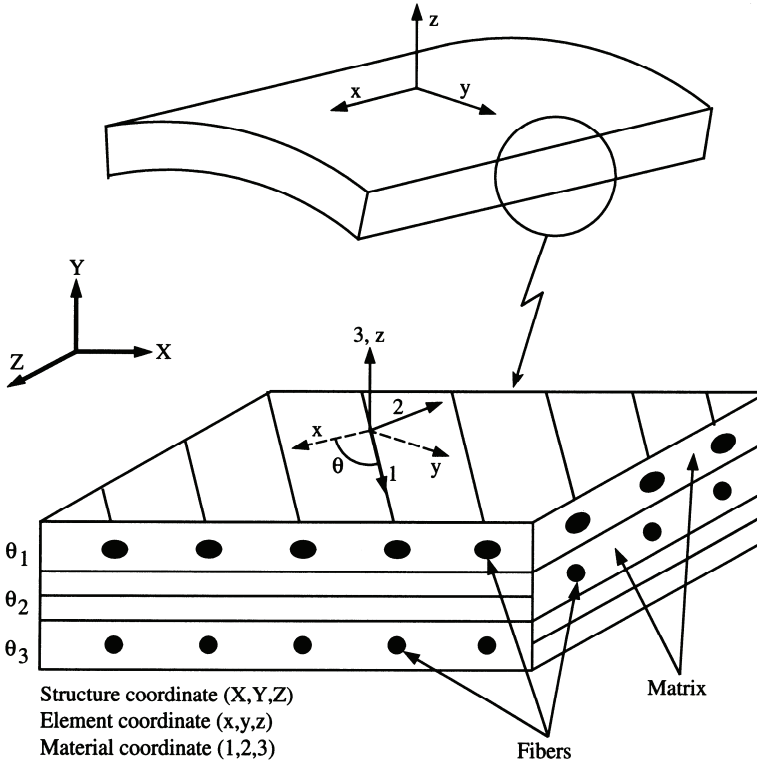


Figure 1: Material, element and structure coordinates of fiber-composite laminated curved panel

$$[Q'_1] = \begin{bmatrix} \frac{E_{11}}{1-\nu_{12}\nu_{21}} & \frac{\nu_{12}E_{22}}{1-\nu_{12}\nu_{21}} & 0 \\ \frac{\nu_{21}E_{11}}{1-\nu_{12}\nu_{21}} & \frac{E_{22}}{1-\nu_{12}\nu_{21}} & 0 \\ 0 & 0 & G_{12} \end{bmatrix} \quad [Q'_2] = \begin{bmatrix} \alpha_1 G_{13} & 0 \\ 0 & \alpha_2 G_{23} \end{bmatrix} \quad (2)$$

where $\{\sigma'\} = \{\sigma_1, \sigma_2, \tau_{12}\}^T$, $\{\tau'\} = \{\tau_{13}, \tau_{23}\}^T$, $\{\varepsilon'\} = \{\varepsilon_1, \varepsilon_2, \gamma_{12}\}^T$, $\{\gamma'\} = \{\gamma_{13}, \gamma_{23}\}^T$. The α_1 and α_2 in Eq. (2) are shear correction factors, which are calculated in Abaqus by assuming that the transverse shear energy through the thickness of laminate is equal to that in unidirectional bending (Whitney, 1973; Abaqus, Inc., 2010). The constitutive equations for the lamina in the element coordinate (x, y, z) then become

$$\{\sigma\} = [Q_1]\{\varepsilon\}, \quad [Q_1] = [T_1]^T [Q'_1] [T_1] \quad (3)$$

$$\{\tau\} = [Q_2]\{\gamma\}, \quad [Q_2] = [T_2]^T [Q'_2] [T_2] \quad (4)$$

$$[T_1] = \begin{bmatrix} \cos^2 \theta & \sin^2 \theta & \sin \theta \cos \theta \\ \sin^2 \theta & \cos^2 \theta & -\sin \theta \cos \theta \\ -2 \sin \theta \cos \theta & 2 \sin \theta \cos \theta & \cos^2 \theta - \sin^2 \theta \end{bmatrix}, \quad [T_2] = \begin{bmatrix} \cos \theta & \sin \theta \\ -\sin \theta & \cos \theta \end{bmatrix} \quad (5)$$

where $\{\sigma\} = \{\sigma_x, \sigma_y, \tau_{xy}\}^T$, $\{\tau\} = \{\tau_{xz}, \tau_{yz}\}^T$, $\{\varepsilon\} = \{\varepsilon_x, \varepsilon_y, \gamma_{xy}\}^T$, $\{\gamma\} = \{\gamma_{xz}, \gamma_{yz}\}^T$, and the fiber orientation θ is measured counterclockwise from the element local x-axis to the material 1-axis.

Let $\{\varepsilon\}_o = \{\varepsilon_{xo}, \varepsilon_{yo}, \varepsilon_{xyo}\}^T$ be the in-plane strains at the mid-surface of the laminate section, $\{\kappa\} = \{\kappa_x, \kappa_y, \kappa_{xy}\}^T$ the curvatures, and h the total thickness of the section. If there are n layers in the laminate section, the stress resultants, $\{N\} = \{N_x, N_y, N_{xy}\}^T$, $\{M\} = \{M_x, M_y, M_{xy}\}^T$ and $\{V\} = \{V_x, V_y\}^T$, can be defined as

$$\begin{Bmatrix} \{N\} \\ \{M\} \\ \{V\} \end{Bmatrix} = \int_{-h/2}^{h/2} \begin{Bmatrix} \{\sigma\} \\ z\{\sigma\} \\ \{\tau\} \end{Bmatrix} dz = \sum_{j=1}^n \begin{bmatrix} (z_{jt} - z_{jb})[Q_1] & \frac{1}{2}(z_{jt}^2 - z_{jb}^2)[Q_1] & [0] \\ \frac{1}{2}(z_{jt}^2 - z_{jb}^2)[Q_1] & \frac{1}{3}(z_{jt}^3 - z_{jb}^3)[Q_1] & [0] \\ [0]^T & [0]^T & (z_{jt} - z_{jb})[Q_2] \end{bmatrix} \begin{Bmatrix} \{\varepsilon_o\} \\ \{\kappa\} \\ \{\gamma\} \end{Bmatrix} \quad (6)$$

The z_{jt} and z_{jb} are the distance from the mid-surface of the section to the top and the bottom of the j -th layer respectively. The $[0]$ is a 3 by 2 matrix with all the coefficients equal to zero.

3 Vibration analysis

For the free vibration analysis of an undamped structure, the equation of motion of the structure can be written in the following form (Cook, Malkus, Plesha and Witt, 2002):

$$[M]\{\ddot{D}\} + [K]\{D\} = \{0\} \quad (7)$$

where $\{D\}$ is a vector for the unrestrained nodal degrees of freedoms, $\{\ddot{D}\}$ an acceleration vector, $[M]$ the mass matrix of the structure, $[K]$ the stiffness matrix of the structure, and $\{0\}$ a zero vector. Since $\{D\}$ undergoes harmonic motion, we can express

$$\{D\} = \{\bar{D}\}\sin\omega t; \quad \{\ddot{D}\} = -\omega^2\{\bar{D}\}\sin\omega t \quad (8)$$

where $\{\bar{D}\}$ vector contains the amplitudes of $\{D\}$ vector. Then Eq. (7) can be written in an eigenvalue expression as

$$([K] - \omega^2[M])\{\bar{D}\} = \{0\} \quad (9)$$

When a laminated curved panel is subjected to compressive force, initial stresses are generated in the panel. Consequently, the stiffness matrix $[K]$ in Eq. (9) can be separated into two matrices as

$$[K] = [K_L] + [K_\sigma] \quad (10)$$

The $[K_L]$ is the traditional linear stiffness matrix and $[K_\sigma]$ is a geometric stress stiffness matrix due to the initial stresses. Then Eq. (9) becomes

$$([K_L] + [K_\sigma] - \omega^2[M])\{\bar{D}\} = \{0\} \quad (11)$$

The preceding equation is an eigenvalue expression. If $\{\bar{D}\}$ is not a zero vector, we must have

$$|[K_L] + [K_\sigma] - \omega^2[M]| = 0 \quad (12)$$

In Abaqus, a subspace iteration procedure (Abaqus, Inc., 2010) is used to solve for the natural frequency ω , and the eigenvectors (or vibration modes) $\{\bar{D}\}$. The obtained smallest natural frequency (fundamental frequency) is then the objective function for maximization.

4 Golden section method

We begin by presenting the golden section method (Vanderplaats, 1984; Haftka, Gürdal and Kamat, 1990) for determining the minimum of the unimodal function F , which is a function of the independent variable \underline{X} . It is assumed that lower bound \underline{X}_L and upper bound \underline{X}_U on \underline{X} are known and the minimum can be bracketed (Fig. 2). In addition, we assume that the function has been evaluated at both bounds and the corresponding values are F_L and F_U . Now we can pick up two intermediate points \underline{X}_1 and \underline{X}_2 such that $\underline{X}_1 < \underline{X}_2$ and evaluate the function at these two points to provide F_1 and F_2 . Because F_1 is greater than F_2 , now \underline{X}_1 forms a new lower bound and we have a new set of bounds, \underline{X}_1 and \underline{X}_U . We can now select an additional point, \underline{X}_3 , for which we evaluate F_3 . It is clear that F_3 is greater than F_2 , so \underline{X}_3 replace \underline{X}_U as the new upper bound. Repeating this process, we can narrow the bounds to whatever tolerance is desired.

To determine the method for choosing the interior points $\underline{X}_1, \underline{X}_2, \underline{X}_3, \dots$, we pick the values of \underline{X}_1 and \underline{X}_2 to be symmetric about the center of the interval and satisfying the following expressions:

$$\underline{X}_U - \underline{X}_2 = \underline{X}_1 - \underline{X}_L \quad (13)$$

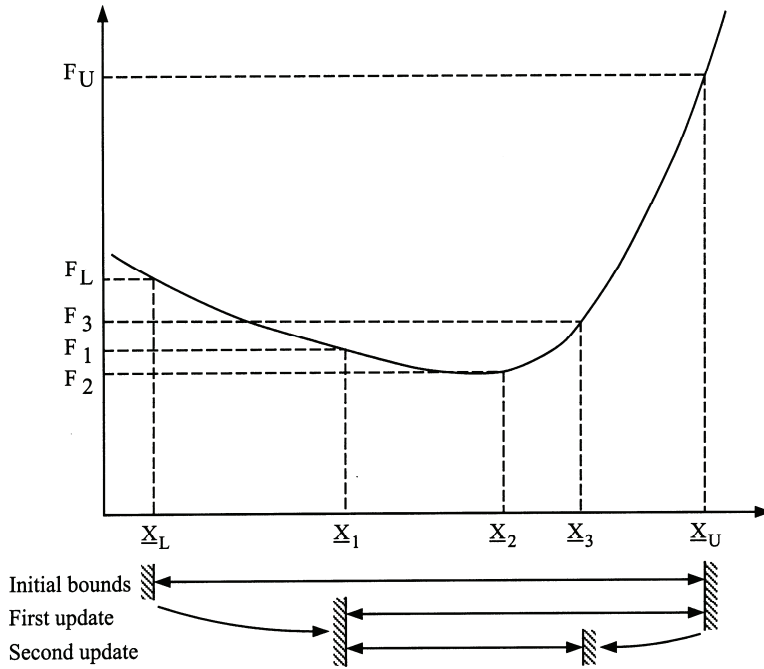


Figure 2: The golden section method

$$\frac{\underline{X}_1 - \underline{X}_L}{\underline{X}_U - \underline{X}_L} = \frac{\underline{X}_2 - \underline{X}_1}{\underline{X}_U - \underline{X}_1} \tag{14}$$

Let τ be a number between 0 and 1. We can define the interior points \underline{X}_1 and \underline{X}_2 to be

$$\underline{X}_1 = (1 - \tau)\underline{X}_L + \tau\underline{X}_U \tag{15a}$$

$$\underline{X}_2 = \tau\underline{X}_L + (1 - \tau)\underline{X}_U \tag{15b}$$

Substituting Eqs. (15a) and (15b) into Eq. (14), we obtain

$$\tau^2 - 3\tau + 1 = 0 \tag{16}$$

Solving the above equation, we obtain $\tau = 0.38197$. The ratio $(1 - \tau)/\tau = 1.61803$ is the famous “golden section” number. For a problem involving the estimation of the maximum of a one-variable function F , we need only minimize the negative of the function, that is, minimize $-F$.

5 Numerical analysis

The accuracy of the eight-node shell element in Abaqus program for frequency analysis has been verified by the authors (Hu and Tsai, 2009; Chen, 2009) and good agreements are obtained between the numerical results and the analytical solution or experimental data. Hence, it is confirmed that the accuracy of the shell element in Abaqus program is good enough to analyze the vibration behavior of laminated curved panels.

5.1 Simply supported laminated curved panels with various curvatures and axial compressive forces

In this section laminated curved panels subjected to axial compressive force N are considered (Fig. 3a). The curved panels are simply supported (denoted by S as shown in Fig. 3b) at the four edges. The simply supported boundary condition prevents out of plane displacement w , but allows in-plane movements u and v .

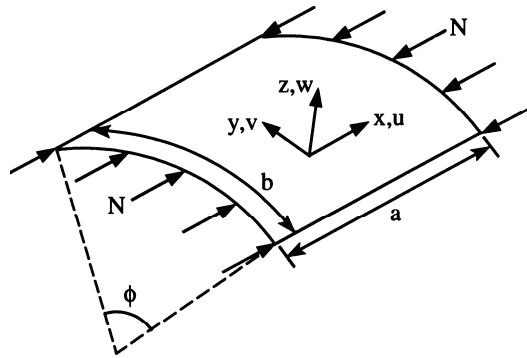
The width b of the curved panel is equal to 10 cm and the circular angle ϕ of the curved panel varies from 5° to 150° . The laminate layup of the curved panel is $[\pm\theta/90/0]_{2s}$ and the thickness of each ply is 0.125 mm. To study the influence of axial compressive force on the results of optimization, $N = 0, 0.2N_{cr}, 0.4N_{cr}, 0.6N_{cr},$ and $0.8N_{cr}$, are selected for analysis, where N_{cr} is the linearized critical buckling load of the laminated curved panel. The lamina consists of Graphite/Epoxy and material constitutive properties are taken from Crawley (1979), which are $E_{11} = 128 \text{ GPa}, E_{22} = 11 \text{ GPa}, G_{23} = 1.53 \text{ GPa}, G_{12} = G_{13} = 4.48 \text{ GPa}, \nu_{12} = 0.25,$ and $\rho = 1500 \text{ kg/m}^3$. In the analysis, no symmetry simplifications are made for those laminated curved panels.

To find the optimal fiber angle θ and the associated optimal fundamental frequency ω , we can express the optimization problem as:

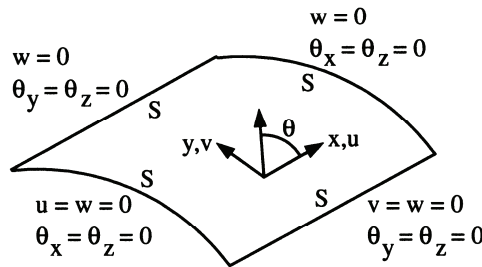
$$\text{Maximize: } \omega(\theta) \tag{17a}$$

$$\text{Subjected to: } 0^\circ \leq \theta \leq 90^\circ \tag{17b}$$

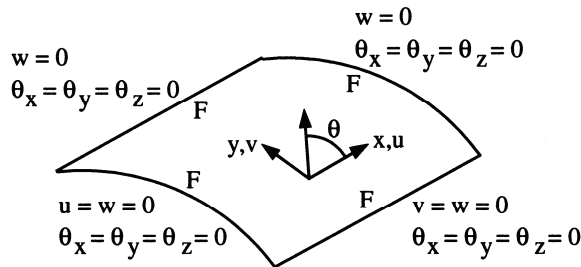
Before the golden section method is carried out, the fundamental frequency ω of the laminated curved panel is calculated by employing the Abaqus finite element program for every 10° increment in θ angle to locate the maximum point approximately. Then proper upper and lower bounds are selected so that the fundamental frequency is a unimodal function within the search region. Finally, the golden section method is carried out to find the maximum. The optimization process is terminated when an absolute tolerance (the difference of the two intermediate points between the upper bound and the lower bound) $\Delta\theta \leq 0.5^\circ$ is reached.



(a) geometry of laminated curved panel



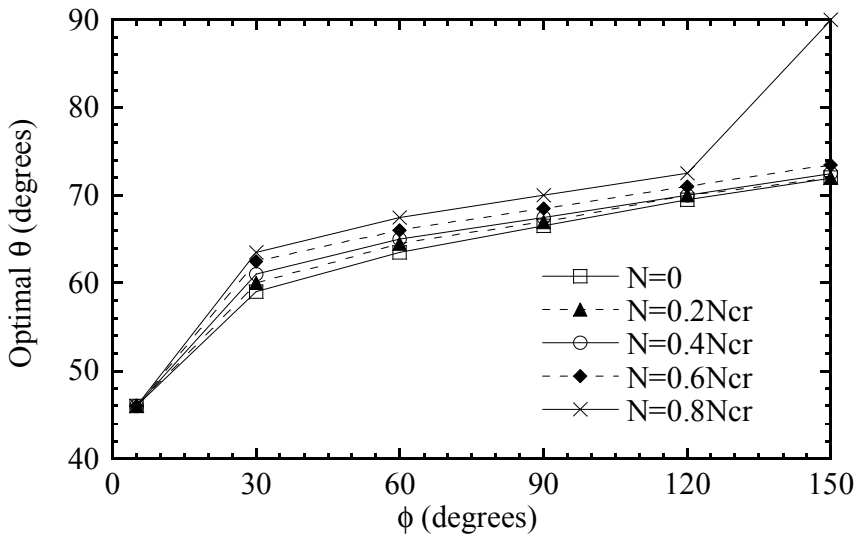
(b) laminated curved panel with simply supported edges



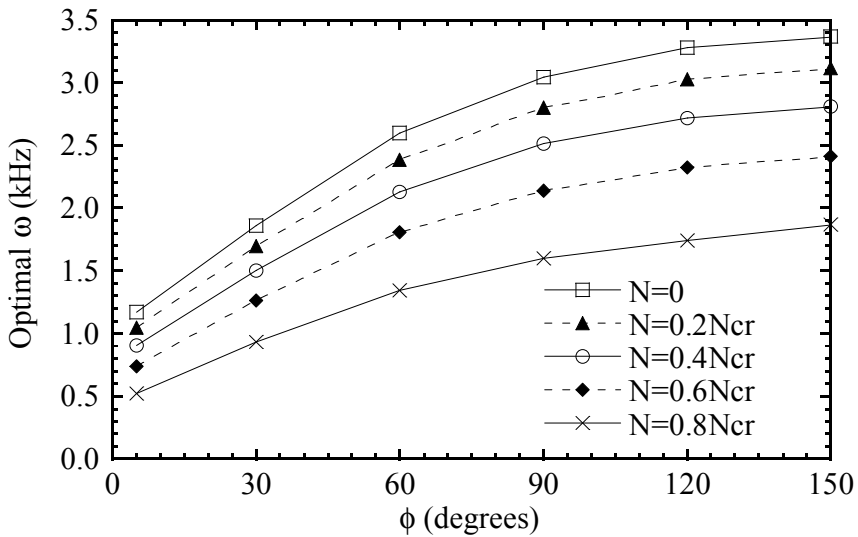
(c) laminated curved panel with fixed edges

Figure 3: Geometry and boundary conditions of laminated curved panels

Figure 4 shows the optimal fiber angle θ and the associated optimal fundamental frequency ω versus the circular angle ϕ for $[\pm\theta/90/0]_{2s}$ laminated curved panel with aspect ratio $a/b = 1$ and with simply supported edge conditions. From Fig. 4a we can see that the axial compressive force N has little influence on the optimal fiber angle θ of the laminated curved panels except the case $\phi = 150^\circ$ and $N = 0.8N_{cr}$. The optimal fiber angle θ of those panels usually varies between 40° and 70° and increases with the increasing of the circular angle ϕ . When $\phi = 5^\circ$, the



(a) Optimal fiber angle θ vs. circular angle ϕ



(b) Optimal fundamental frequency ω vs. circular angle ϕ

Figure 4: Effect of curvature and in-plane compressive force on optimal fiber angle and optimal fundamental frequency of $[\pm\theta/90/0]_{2s}$ laminated curved panels with four simply supported edges ($b = 10$ cm, $a/b = 1$)

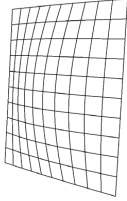
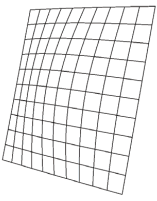
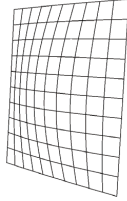
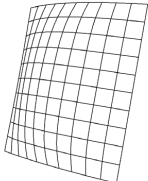
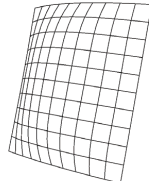
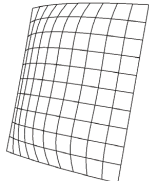
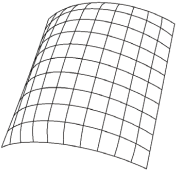
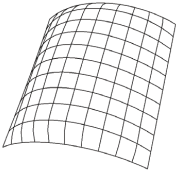
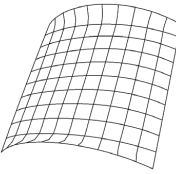
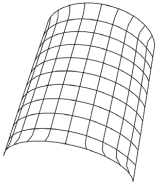
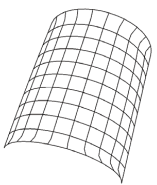
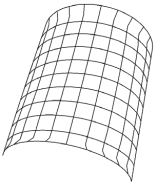
ϕ	$N = 0$	$N = 0.4N_{cr}$	$N = 0.8N_{cr}$
5°	 $\theta = 46^\circ$ $\omega = 1172 \text{ Hz}$	 $\theta = 46^\circ$ $\omega = 908 \text{ Hz}$	 $\theta = 46^\circ$ $\omega = 523 \text{ Hz}$
30°	 $\theta = 59^\circ$ $\omega = 1862 \text{ Hz}$	 $\theta = 61^\circ$ $\omega = 1503 \text{ Hz}$	 $\theta = 63.5^\circ$ $\omega = 932 \text{ Hz}$
90°	 $\theta = 66.5^\circ$ $\omega = 3046 \text{ Hz}$	 $\theta = 67.5^\circ$ $\omega = 2514 \text{ Hz}$	 $\theta = 70^\circ$ $\omega = 1599 \text{ Hz}$
150°	 $\theta = 72^\circ$ $\omega = 3368 \text{ Hz}$	 $\theta = 72.5^\circ$ $\omega = 2811 \text{ Hz}$	 $\theta = 90^\circ$ $\omega = 1872 \text{ Hz}$

Figure 5: Fundamental vibration modes of $[\pm\theta/90/0]_{2s}$ laminated curved panels with four simply supported edges and under optimal fiber angles ($b = 10 \text{ cm}$, $a/b = 1$)

optimal fiber angle θ of the laminated curved panels are all equal to 46° and seem to be independent on the axial compressive forces. Figure 4b shows that the optimal fundamental frequency ω increases with the increasing of the circular angle ϕ . However, it decreases with the increasing of the axial compressive force. Figure 5 shows that the fundamental vibration modes of those curved panels with $a/b = 1$ under optimal fiber angle θ . It can be seen that those modes are very similar and all of them have a half sine wave in both axial direction (x-axis in Fig. 3) and circumferential direction (y-axis in Fig. 3).

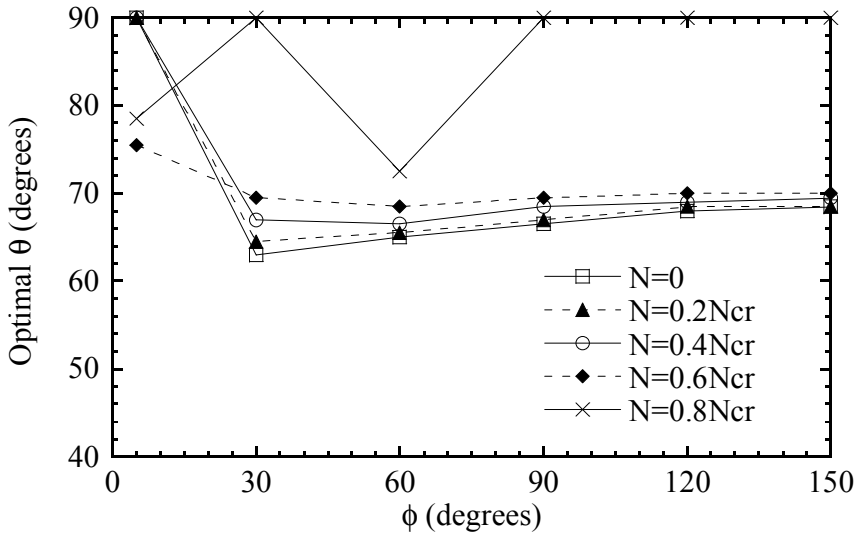
Figure 6 shows the optimal fiber angle θ and the associated optimal fundamental frequency ω versus the circular angle ϕ for $[\pm\theta/90/0]_{2s}$ laminated curved panel with aspect ratio $a/b = 2$ and with simply supported edge conditions. From Fig. 6a we can see that when the axial force $N \leq 0.6N_{cr}$ and $\theta < 60^\circ$ (especially $\theta < 30^\circ$), the axial force has significant influence on the optimal fiber angle. For the panels with $N \leq 0.6N_{cr}$, when the circular angle ϕ is large, the optimal fiber angle tends to approach 70° . However, for the panels with $N = 0.8N_{cr}$ and $\phi \geq 30^\circ$ the optimal fiber angle tends to approach 90° (the exception is the panel with $\phi = 60^\circ$ where the optimal fiber angle is 72.5°).

Figure 6b again shows that the optimal fundamental frequency ω increases with the increasing of the circular angle ϕ and decreases with the increasing of the axial compressive force N . Comparing Fig. 6a with Fig. 4a, we can see that the aspect ratio a/b has significant influence on the optimal fiber angle of the laminated curved panel. Comparing Fig. 6b with Fig. 4b, we can see that the optimal fundamental frequencies of the curved panels with small aspect ratio are greater than those with large aspect ratio.

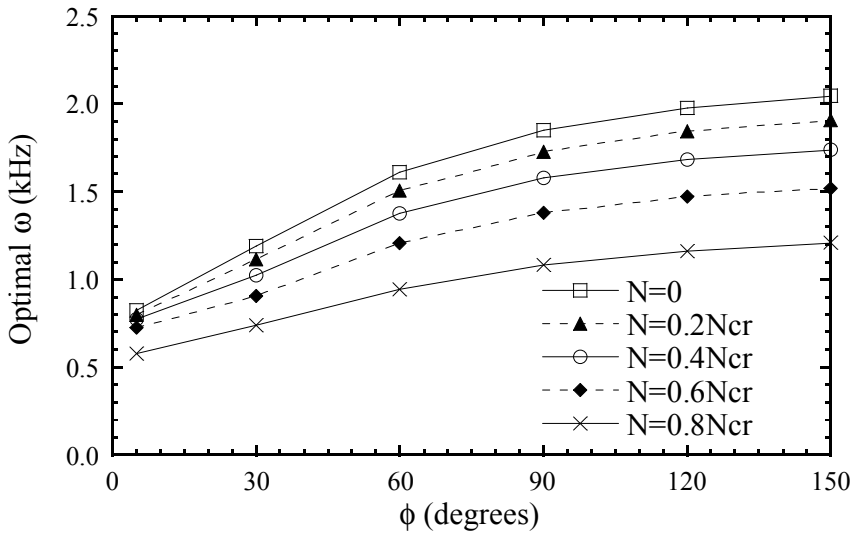
Figure 7 shows the fundamental vibration modes of those curved panels with $a/b = 2$ under optimal fiber angle θ . Comparing Fig. 7 with Fig. 5, it is observed when the curved panel has large aspect ratio (say $a/b = 2$), small circular angle (say $\phi = 5^\circ$) and subjected to large compressive force (say $N = 0.8N_{cr}$), its vibration mode under optimal fiber angle may have more half sine wave numbers in the axial direction.

5.2 Fixed laminated curved panels with various curvatures and axial compressive forces

In this section, laminated curved panels subjected to axial compressive force and similar to those in previous section are analyzed except that the panels are fixed (denoted by F as shown in Fig. 3c) at the four edges. The fixed boundary condition also prevents out of plane displacement w , but allows in-plane movements u and v . The laminate layup of the laminated curved panel is still $[\pm\theta/90/0]_{2s}$.



(a) Optimal fiber angle θ vs. circular angle ϕ



(b) Optimal fundamental frequency ω vs. circular angle ϕ

Figure 6: Effect of curvature and in-plane compressive force on optimal fiber angle and optimal fundamental frequency of $[\pm\theta/90/0]_{2s}$ laminated curved panels with four simply supported edges ($b = 10$ cm, $a/b = 2$)







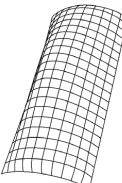
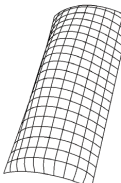
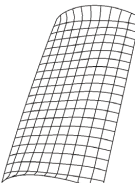
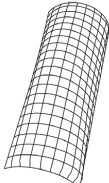
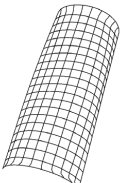
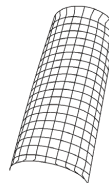
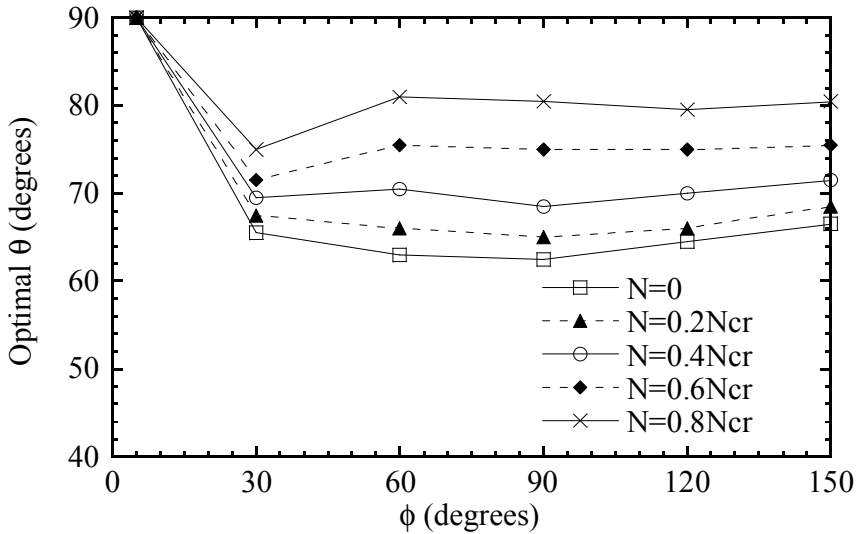
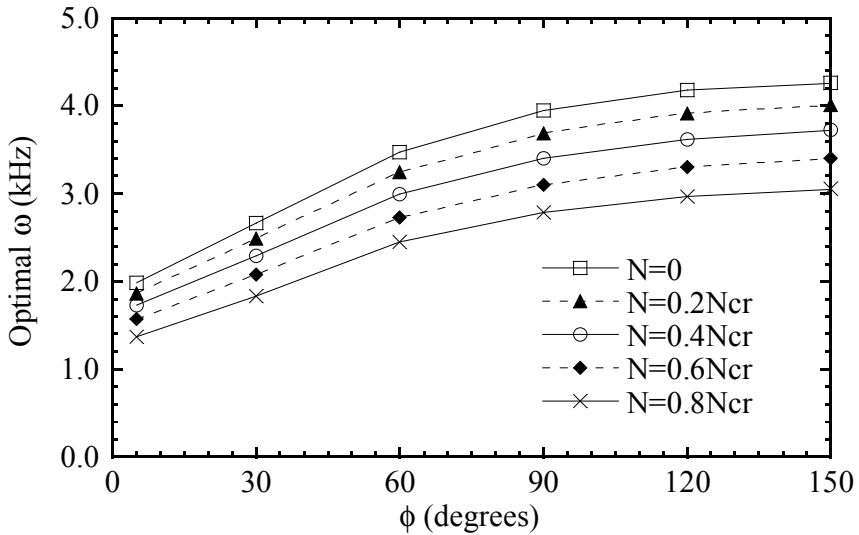
ϕ	$N = 0$	$N = 0.4N_{cr}$	$N = 0.8N_{cr}$
5°	 $\theta = 90^\circ$ $\omega = 823 \text{ Hz}$	 $\theta = 90^\circ$ $\omega = 773 \text{ Hz}$	 $\theta = 78.5^\circ$ $\omega = 578 \text{ Hz}$
30°	 $\theta = 63^\circ$ $\omega = 1192 \text{ Hz}$	 $\theta = 67^\circ$ $\omega = 1023 \text{ Hz}$	 $\theta = 90^\circ$ $\omega = 738 \text{ Hz}$
90°	 $\theta = 66.5^\circ$ $\omega = 1849 \text{ Hz}$	 $\theta = 68.5^\circ$ $\omega = 1578 \text{ Hz}$	 $\theta = 90^\circ$ $\omega = 1085 \text{ Hz}$
150°	 $\theta = 68.5^\circ$ $\omega = 2045 \text{ Hz}$	 $\theta = 69.5^\circ$ $\omega = 1740 \text{ Hz}$	 $\theta = 90^\circ$ $\omega = 1210 \text{ Hz}$

Figure 7: Fundamental vibration modes of $[\pm\theta/90/0]_{2s}$ laminated curved panels with four simply supported edges and under optimal fiber angles ($b = 10 \text{ cm}$, $a/b = 2$)



(a) Optimal fiber angle θ vs. circular angle ϕ



(b) Optimal fundamental frequency ω vs. circular angle ϕ

Figure 8: Effect of curvature and in-plane compressive force on optimal fiber angle and optimal fundamental frequency of $[\pm\theta/90/0]_{2s}$ laminated curved panels with four fixed edges ($b = 10$ cm, $a/b = 1$)

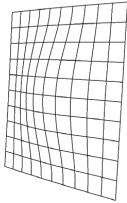
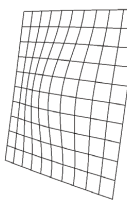
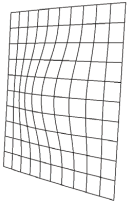



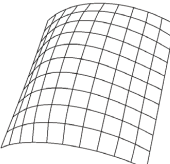
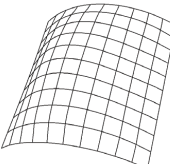
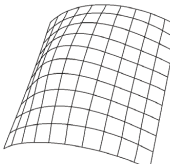
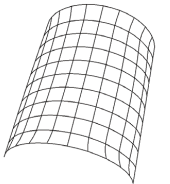
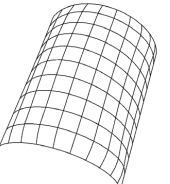
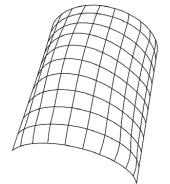
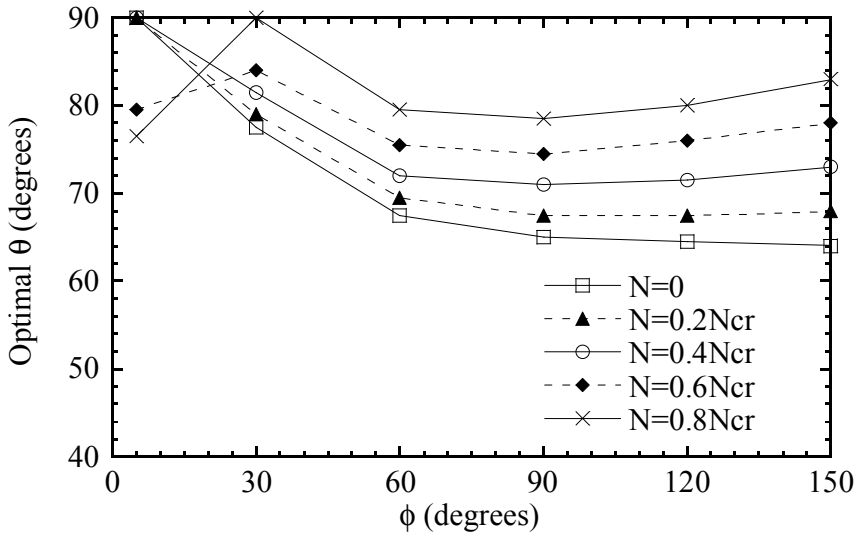
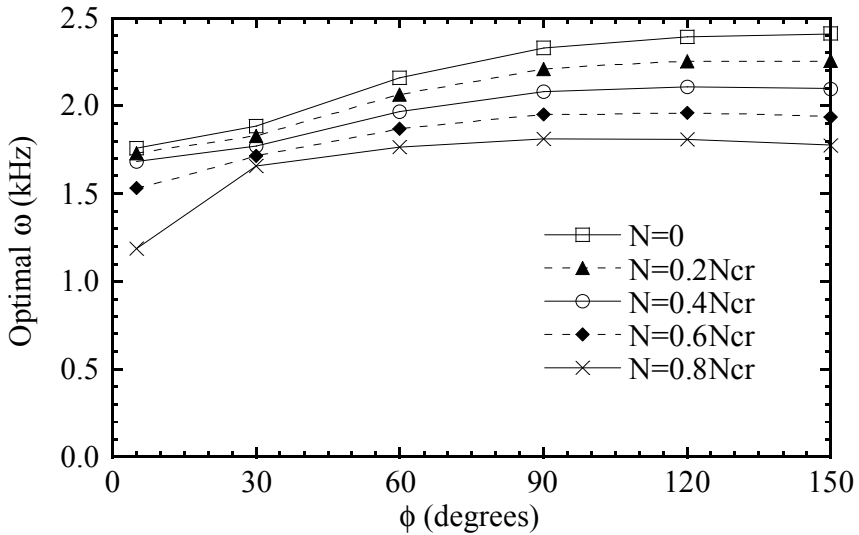
ϕ	$N = 0$	$N = 0.4N_{cr}$	$N = 0.8N_{cr}$
5°	 $\theta = 90^\circ$ $\omega = 1984 \text{ Hz}$	 $\theta = 90^\circ$ $\omega = 1731 \text{ Hz}$	 $\theta = 90^\circ$ $\omega = 1367 \text{ Hz}$
30°	 $\theta = 65.5^\circ$ $\omega = 2668 \text{ Hz}$	 $\theta = 69.5^\circ$ $\omega = 2292 \text{ Hz}$	 $\theta = 75^\circ$ $\omega = 1828 \text{ Hz}$
90°	 $\theta = 62.5^\circ$ $\omega = 3946 \text{ Hz}$	 $\theta = 68.5^\circ$ $\omega = 3402 \text{ Hz}$	 $\theta = 80.5^\circ$ $\omega = 2781 \text{ Hz}$
150°	 $\theta = 66.5^\circ$ $\omega = 4265 \text{ Hz}$	 $\theta = 71.5^\circ$ $\omega = 3723 \text{ Hz}$	 $\theta = 80.5^\circ$ $\omega = 3058 \text{ Hz}$

Figure 9: Fundamental vibration modes of $[\pm\theta/90/0]_{2s}$ laminated curved panels with four fixed edges and under optimal fiber angles ($b = 10 \text{ cm}$, $a/b = 1$)



(a) Optimal fiber angle θ vs. circular angle ϕ



(b) Optimal fundamental frequency ω vs. circular angle ϕ

Figure 10: Effect of curvature and in-plane compressive force on optimal fiber angle and optimal fundamental frequency of $[\pm\theta/90/0]_{2s}$ laminated curved panels with four fixed edges ($b = 10$ cm, $a/b = 2$)

Figure 8 shows the optimal fiber angle θ and the associated optimal fundamental frequency ω versus the circular angle ϕ for $[\pm\theta/90/0]_{2s}$ laminated curved panel with aspect ratio $a/b = 1$ and with fixed edge conditions. From Fig. 8a we can see that the axial compressive force N does have some influence on the optimal fiber angle θ of the laminated curved panels when the circular angle is large (say $\phi \geq 30^\circ$). The optimal fiber angle increases with the increasing of the compressive force and usually varies between 60° and 90° . Similar to the panels with four simply supported edges (Fig. 4a), when $\phi = 5^\circ$, the optimal fiber angle θ of the laminated curved panels are all equal to 90° and seem to be independent on the axial compressive forces. Figure 8b shows that the optimal fundamental frequency ω increases with the increasing of the circular angle ϕ . However, it decreases with the increasing of the axial compressive force. Figure 9 shows the fundamental vibration modes of those curved panels with $a/b = 1$ and under optimal fiber angle θ . It can be seen that those modes are very similar.

Figure 10 shows the optimal fiber angle θ and the associated optimal fundamental frequency ω versus the circular angle ϕ for $[\pm\theta/90/0]_{2s}$ laminated curved panel with aspect ratio $a/b = 2$ and with fixed edge conditions. From Fig. 10a we can see that the axial compressive force N does have some influence on the optimal fiber angle θ of the laminated curved panels. The optimal fiber angle θ of those panels usually varies between 60° and 90° . Figure 10b shows that the optimal fundamental frequency ω increases with the increasing of the circular angle ϕ and decreases with the increasing of the axial compressive force. Comparing Fig. 10 with Fig. 8, we can see that the aspect ratio a/b has significant influence on the optimal fiber angle and optimal fundamental frequency of the curved panel. Finally, comparing Figs. 8 and 10 with Figs. 4 and 6, we can conclude that the boundary condition has significant influence on the optimal fiber angle and the associated optimal fundamental frequency of the laminated curved panels.

Figure 11 shows the fundamental vibration modes of those curved panels with $a/b = 2$ and under optimal fiber angle θ . Comparing Fig. 11 with Fig. 9, it is observed when the curved panel has large aspect ratio (say $a/b = 2$), small circular angle (say $\phi = 5^\circ$) and subjected to large compressive force (say $N \geq 0.4N_{cr}$), its vibration mode under optimal fiber angle may have more wave numbers in the axial direction.

5.3 Simply supported laminated curved panels with various aspect ratios and axial compressive forces

In this section, laminated curved panels subjected to axial compressive force are analyzed. The width b of the curved panel is equal to 10 cm and the length a of the curved panel varies from 5 cm to 20 cm. The panels are simply supported at the four edges. The laminate layup of the laminated curved panel is still $[\pm\theta/90/0]_{2s}$.







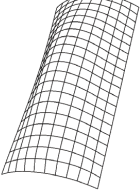
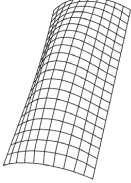
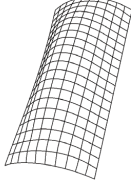
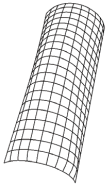
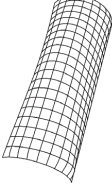
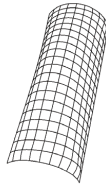
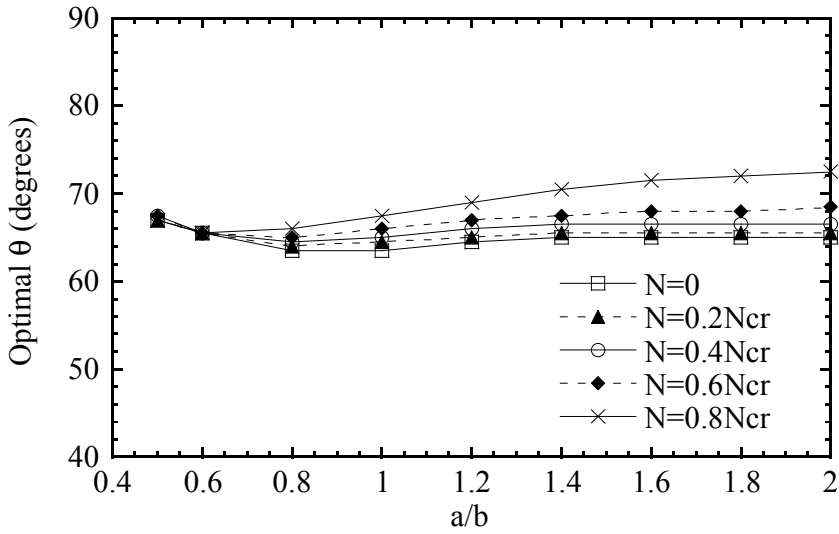
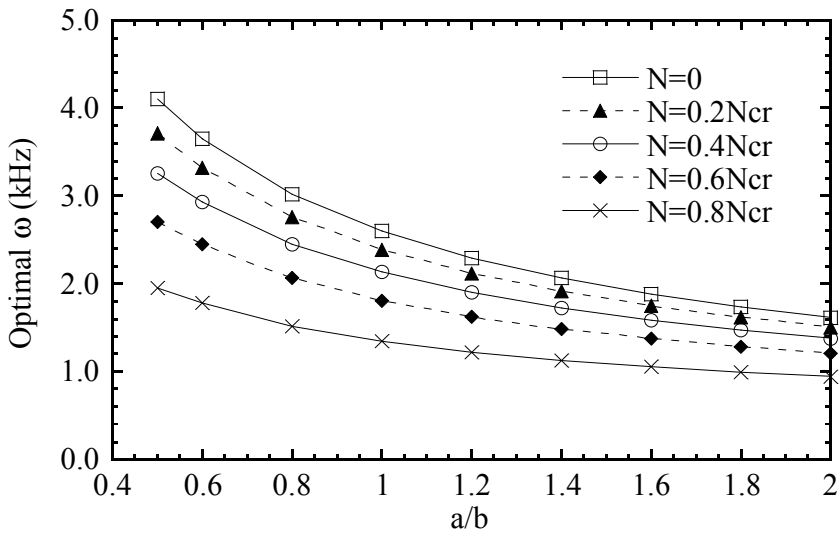
ϕ	$N = 0$	$N = 0.4N_{cr}$	$N = 0.8N_{cr}$
5°	 $\theta = 90^\circ$ $\omega = 1757 \text{ Hz}$	 $\theta = 90^\circ$ $\omega = 1681 \text{ Hz}$	 $\theta = 76.5^\circ$ $\omega = 1187 \text{ Hz}$
30°	 $\theta = 77.5^\circ$ $\omega = 1883 \text{ Hz}$	 $\theta = 81.5^\circ$ $\omega = 1773 \text{ Hz}$	 $\theta = 90^\circ$ $\omega = 1657 \text{ Hz}$
90°	 $\theta = 65^\circ$ $\omega = 2329 \text{ Hz}$	 $\theta = 71^\circ$ $\omega = 2082 \text{ Hz}$	 $\theta = 78.5^\circ$ $\omega = 1813 \text{ Hz}$
150°	 $\theta = 64^\circ$ $\omega = 2413 \text{ Hz}$	 $\theta = 73^\circ$ $\omega = 2096 \text{ Hz}$	 $\theta = 83^\circ$ $\omega = 1775 \text{ Hz}$

Figure 11: Fundamental vibration modes of $[\pm\theta/90/0]_{2s}$ laminated curved panels with four fixed edges and under optimal fiber angles ($b = 10 \text{ cm}$, $a/b = 2$)



(a) Optimal fiber angle θ vs. aspect ratio a/b



(b) Optimal fundamental frequency ω vs. aspect ratio a/b

Figure 12: Effect of aspect ratio and in-plane compressive force on optimal fiber angle and optimal fundamental frequency of $[\pm\theta/90/0]_{2s}$ laminated curved panels with four simply supported edges ($b = 10$ cm, $\phi = 60^\circ$)

Figure 12 shows the optimal fiber angle θ and the associated optimal fundamental frequency ω versus aspect ratio a/b for $[\pm\theta/90/0]_{2s}$ laminated curved panels with $\phi = 60^\circ$ and with simply supported conditions. From Fig. 12a we can see that the axial compressive force N does have some influence on the optimal fiber angle θ of the laminated curved panels when the aspect ratio is large (say $a/b \geq 0.8$). The optimal fiber angle increases with the increasing of the compressive force and usually varies between 60° and 70° . When $a/b = 0.5$, the optimal fiber angle θ of the laminated curved panels are all equal to 67° and seem to be independent on the axial compressive forces. Figure 12b shows that the optimal fundamental frequency ω decreases with the increasing of the aspect ratio a/b and decreases with the increasing of the axial compressive force. Figure 13 shows the fundamental vibration modes of those curved panels with $\phi = 60^\circ$ and under optimal fiber angle θ . Again, it can be seen that those modes are very similar.

Figure 14 shows the optimal fiber angle θ and the associated optimal fundamental frequency ω versus the circular angle ϕ for $[\pm\theta/90/0]_{2s}$ laminated curved panel with $\phi = 150^\circ$ and with simply supported edge conditions. From Fig. 14a we can see that the axial compressive force N has little influences on the optimal fiber angle θ of the laminated curved panels when the aspect ratio is large (say $a/b \geq 0.8$). The optimal fiber angle θ of those panels usually varies between 70° and 90° . When the aspect ratio is large, the optimal fiber angle tends to approach constant value. Figure 14b shows again that the optimal fundamental frequency ω decreases with the increasing of the aspect ratio a/b and decreases with the increasing of the axial compressive force. Comparing Fig. 14a with Fig. 12a, we can see that the circular angle ϕ has significant influence on the optimal fiber angle of the laminated curved panel. Comparing Fig. 14b with Fig. 12b, we can see that the optimal fundamental frequencies of the curved panels with small circular angle are smaller than those with large circular angle. Figure 15 shows the fundamental vibration modes of those curved panels with $\phi = 150^\circ$ under optimal fiber angle θ . Again, it can be seen that those modes are very similar.

5.4 Fixed laminated curved panels with various aspect ratios and axial compressive forces

In this section, laminated curved panels subjected to axial compressive force and similar to those in previous section are analyzed except that the panels are fixed at the four edges. The laminate layup of the laminated curved panel is still $[\pm\theta/90/0]_{2s}$. Figure 16 shows the optimal fiber angle θ and the associated optimal fundamental frequency ω versus aspect ratio a/b for $[\pm\theta/90/0]_{2s}$ laminated curved panels with $\phi = 60^\circ$ and with fixed conditions. From Fig. 16a we can see that the axial compressive force N does have some influence on the optimal fiber angle θ of

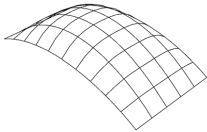
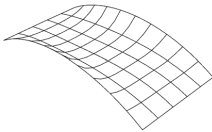
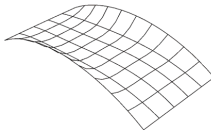
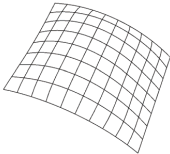
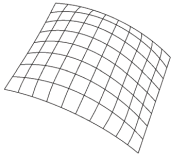
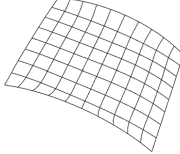
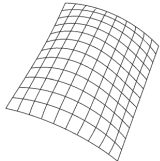
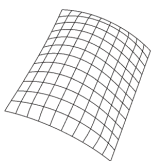
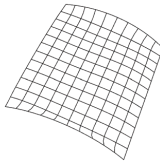
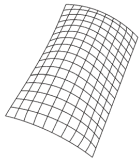
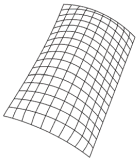
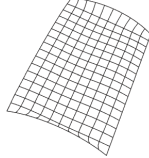
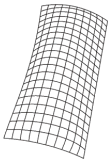
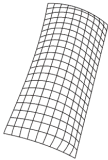
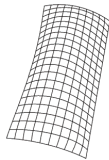
a/b	$N = 0$	$N = 0.4N_{cr}$	$N = 0.8N_{cr}$
0.5	 <p>$\theta = 67^\circ$ $\omega = 4103$ Hz</p>	 <p>$\theta = 67.5^\circ$ $\omega = 3259$ Hz</p>	 <p>$\theta = 67^\circ$ $\omega = 1952$ Hz</p>
0.8	 <p>$\theta = 63.5^\circ$ $\omega = 3022$ Hz</p>	 <p>$\theta = 64.5^\circ$ $\omega = 2453$ Hz</p>	 <p>$\theta = 66^\circ$ $\omega = 1518$ Hz</p>
1.2	 <p>$\theta = 64.5^\circ$ $\omega = 2295$ Hz</p>	 <p>$\theta = 66^\circ$ $\omega = 1901$ Hz</p>	 <p>$\theta = 69^\circ$ $\omega = 1220$ Hz</p>
1.6	 <p>$\theta = 65^\circ$ $\omega = 1884$ Hz</p>	 <p>$\theta = 66.5^\circ$ $\omega = 1587$ Hz</p>	 <p>$\theta = 71.5^\circ$ $\omega = 1053$ Hz</p>
2	 <p>$\theta = 65^\circ$ $\omega = 1611$ Hz</p>	 <p>$\theta = 66.5^\circ$ $\omega = 1376$ Hz</p>	 <p>$\theta = 72.5^\circ$ $\omega = 943$ Hz</p>

Figure 13: Fundamental vibration modes of $[\pm\theta/90/0]_{2s}$ laminated curved panels with four simply supported edges and under optimal fiber angles ($b = 10$ cm, $\phi = 60^\circ$)

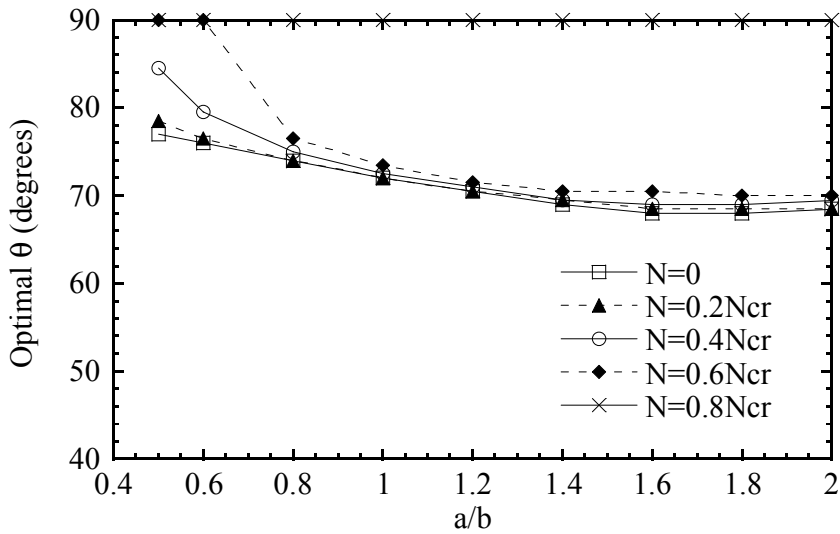
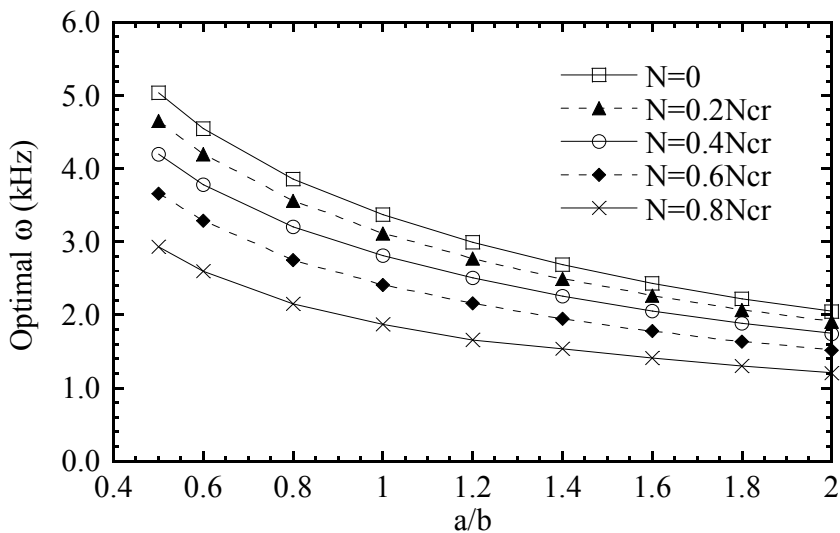
(a) Optimal fiber angle θ vs. aspect ratio a/b (b) Optimal fundamental frequency ω vs. aspect ratio a/b

Figure 14: Effect of aspect ratio and in-plane compressive force on optimal fiber angle and optimal fundamental frequency of $[\pm\theta/90/0]_{2s}$ laminated curved panels with four simply supported edges ($b = 10$ cm, $\phi = 150^\circ$)

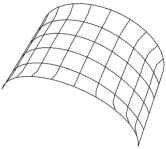
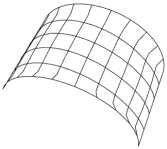
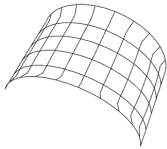
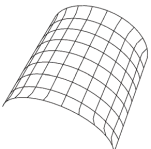
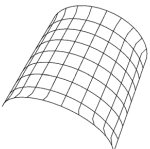
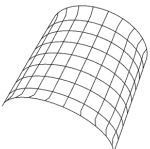
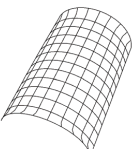
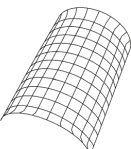
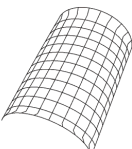
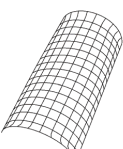
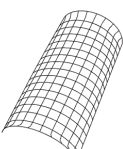
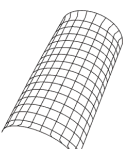
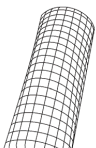
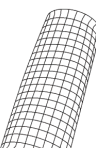
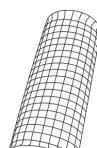
a/b	$N = 0$	$N = 0.4N_{cr}$	$N = 0.8N_{cr}$
0.5	 $\theta = 77^\circ$ $\omega = 5035 \text{ Hz}$	 $\theta = 84.5^\circ$ $\omega = 4195 \text{ Hz}$	 $\theta = 90^\circ$ $\omega = 2937 \text{ Hz}$
0.8	 $\theta = 74^\circ$ $\omega = 3855 \text{ Hz}$	 $\theta = 75^\circ$ $\omega = 3210 \text{ Hz}$	 $\theta = 90^\circ$ $\omega = 2154 \text{ Hz}$
1.2	 $\theta = 70.5^\circ$ $\omega = 2994 \text{ Hz}$	 $\theta = 71^\circ$ $\omega = 2506 \text{ Hz}$	 $\theta = 90^\circ$ $\omega = 1657 \text{ Hz}$
1.6	 $\theta = 68^\circ$ $\omega = 2436 \text{ Hz}$	 $\theta = 69^\circ$ $\omega = 2056 \text{ Hz}$	 $\theta = 90^\circ$ $\omega = 1409 \text{ Hz}$
2	 $\theta = 68.5^\circ$ $\omega = 2045 \text{ Hz}$	 $\theta = 69.5^\circ$ $\omega = 1740 \text{ Hz}$	 $\theta = 90^\circ$ $\omega = 1210 \text{ Hz}$

Figure 15: Fundamental vibration modes of $[\pm\theta/90/0]_{2s}$ laminated curved panels with four simply supported edges and under optimal fiber angles ($b = 10 \text{ cm}$, $\phi = 150^\circ$)

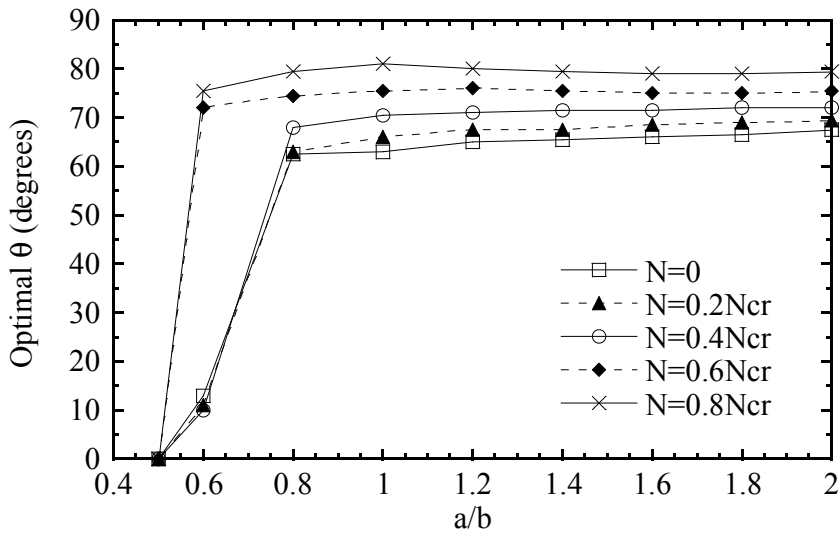
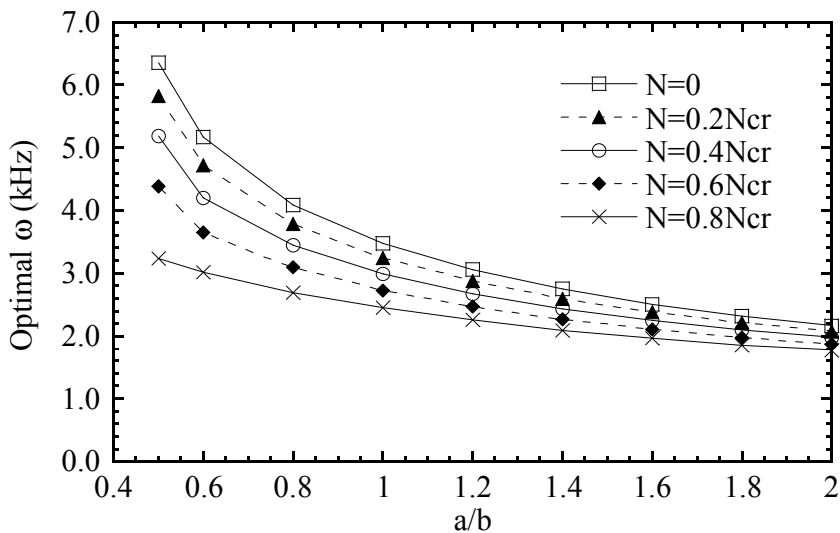
(a) Optimal fiber angle θ vs. aspect ratio a/b (b) Optimal fundamental frequency ω vs. aspect ratio a/b

Figure 16: Effect of aspect ratio and in-plane compressive force on optimal fiber angle and optimal fundamental frequency of $[\pm\theta/90/0]_{2s}$ laminated curved panels with four fixed edges ($b = 10$ cm, $\phi = 60^\circ$)

the laminated curved panels when the aspect ratio is large (say $a/b \geq 0.6$). The optimal fiber angle increases with the increasing of the compressive force and usually varies between 0° and 80° . When the aspect ratio is large, the optimal fiber angle tends to approach constant value. Similar to the panels with four simply supported edges (Fig. 12a), when $a/b = 0.5$, the optimal fiber angle θ of the laminated curved panels are all equal to 0° and seem to be independent on the axial compressive forces. Figure 16b shows that the optimal fundamental frequency ω decreases with the increasing of the aspect ratio a/b and decreases with the increasing of the axial compressive force. Figure 17 shows the fundamental vibration modes of those curved panels with $\phi = 60^\circ$ and under optimal fiber angle θ . It can be seen the fundamental vibration modes of the panels under optimal fiber angle are very similar.

Figure 18 shows the optimal fiber angle θ and the associated optimal fundamental frequency ω versus the circular angle ϕ for $[\pm\theta/90/0]_2$, laminated curved panel with $\phi = 150^\circ$ and with fixed edge conditions. From Fig. 18a we can see that the axial compressive force N has significant influences on the optimal fiber angle θ of the laminated curved panels. The optimal fiber angle θ of those panels usually varies between 60° and 90° . Figure 18b shows again that the optimal fundamental frequency ω decreases with the increasing of the aspect ratio a/b and decreases with the increasing of the axial compressive force. Comparing Fig. 18a with Fig. 16a, we can see that the circular angle ϕ has significant influence on the optimal fiber angle of the laminated curved panel. Comparing Fig. 18b with Fig. 16b, we can see that the optimal fundamental frequencies of the curved panels with small circular angle are smaller than those with large circular angle. Finally, comparing Figs. 16 and 18 with Figs. 12 and 14, we can conclude that the boundary condition has significant influence on the optimal fiber angle and the associated optimal fundamental frequency of the laminated curved panels. Figure 19 shows the fundamental vibration modes of those curved panels with $\phi = 150^\circ$ under optimal fiber angle θ . Again, it can be seen the fundamental vibration modes of the panels under optimal fiber angle are very similar.

6 Conclusions

Generally, the axial compressive force, curvature, aspect ratio and boundary conditions have significant influence on the optimal fiber angle and the associated optimal fundamental frequency of laminated curved panels. Based on the numerical results of this investigation, the following specific conclusions may be drawn:

1. The optimal fundamental frequency ω of the curved laminated panel increases with the increasing of the circular angle ϕ and decreases with the increasing of the axial compressive force.

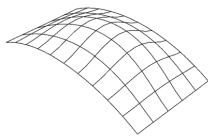
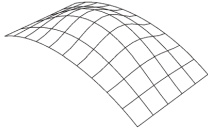
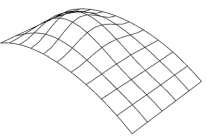
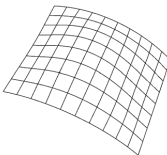
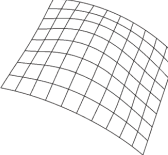
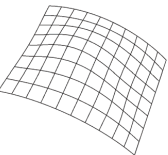
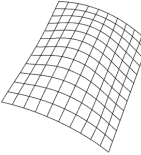
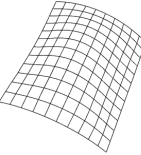
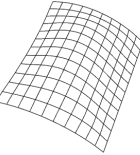
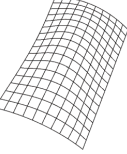
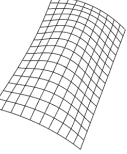
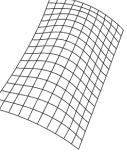
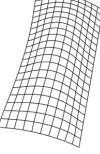
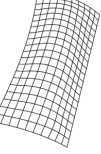
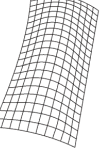
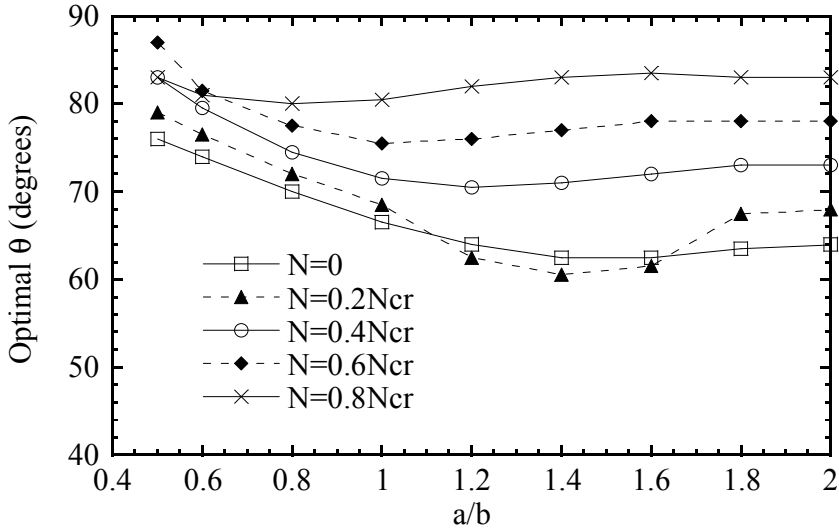
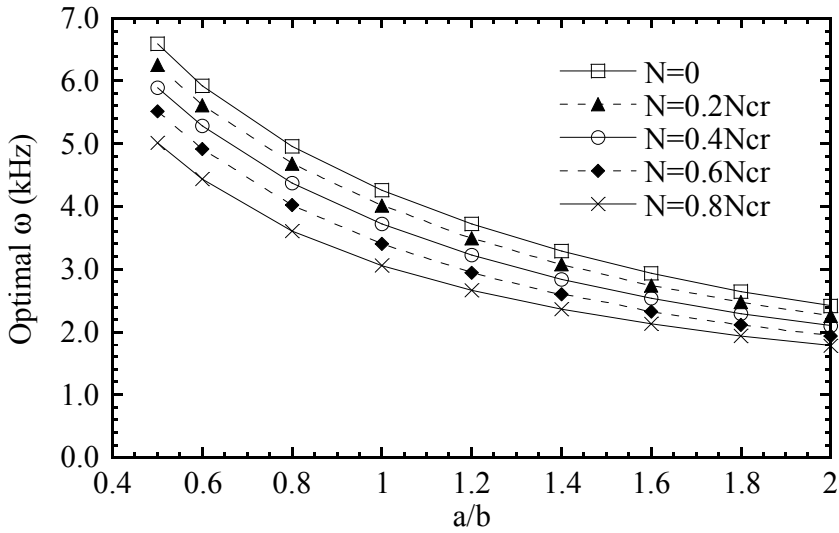
a/b	$N = 0$	$N = 0.4N_{cr}$	$N = 0.8N_{cr}$
0.5	 $\theta = 0^\circ$ $\omega = 6361$ Hz	 $\theta = 0^\circ$ $\omega = 5186$ Hz	 $\theta = 0^\circ$ $\omega = 3240$ Hz
0.8	 $\theta = 62.5^\circ$ $\omega = 4085$ Hz	 $\theta = 68^\circ$ $\omega = 3453$ Hz	 $\theta = 79.5^\circ$ $\omega = 2688$ Hz
1.2	 $\theta = 65^\circ$ $\omega = 3055$ Hz	 $\theta = 71^\circ$ $\omega = 2672$ Hz	 $\theta = 80^\circ$ $\omega = 2251$ Hz
1.6	 $\theta = 66^\circ$ $\omega = 2507$ Hz	 $\theta = 71.5^\circ$ $\omega = 2244$ Hz	 $\theta = 79^\circ$ $\omega = 1959$ Hz
2	 $\theta = 67.5^\circ$ $\omega = 2160$ Hz	 $\theta = 72^\circ$ $\omega = 1968$ Hz	 $\theta = 79.5^\circ$ $\omega = 1766$ Hz

Figure 17: Fundamental vibration modes of $[\pm\theta/90/0]_{2s}$ laminated curved panels with four fixed edges and under optimal fiber angles ($b = 10$ cm, $\phi = 60^\circ$)



(a) Optimal fiber angle θ vs. aspect ratio a/b



(b) Optimal fundamental frequency ω vs. aspect ratio a/b

Figure 18: Effect of aspect ratio and in-plane compressive force on optimal fiber angle and optimal fundamental frequency of $[\pm\theta/90/0]_{2s}$ laminated curved panels with four fixed edges ($b = 10$ cm, $\phi = 150^\circ$)

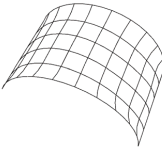
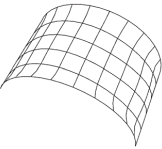
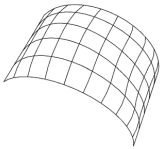
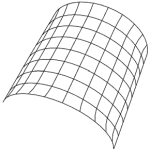
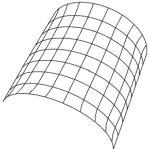
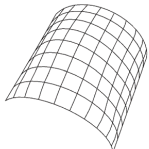
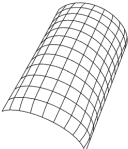
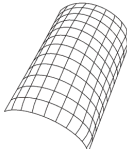
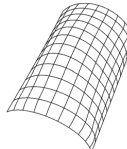
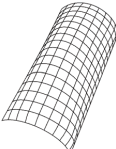
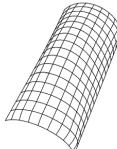
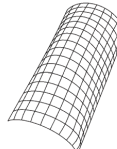
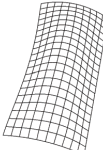
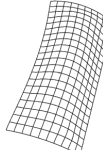
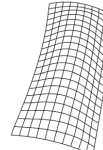
a/b	$N = 0$	$N = 0.4N_{cr}$	$N = 0.8N_{cr}$
0.5	 $\theta = 76^\circ$ $\omega = 6591 \text{ Hz}$	 $\theta = 83^\circ$ $\omega = 5901 \text{ Hz}$	 $\theta = 93^\circ$ $\omega = 5014 \text{ Hz}$
0.8	 $\theta = 70^\circ$ $\omega = 4959 \text{ Hz}$	 $\theta = 74.5^\circ$ $\omega = 4376 \text{ Hz}$	 $\theta = 80^\circ$ $\omega = 3610 \text{ Hz}$
1.2	 $\theta = 64^\circ$ $\omega = 3723 \text{ Hz}$	 $\theta = 70.5^\circ$ $\omega = 3225 \text{ Hz}$	 $\theta = 82^\circ$ $\omega = 2661 \text{ Hz}$
1.6	 $\theta = 63.5^\circ$ $\omega = 2933 \text{ Hz}$	 $\theta = 72^\circ$ $\omega = 2535 \text{ Hz}$	 $\theta = 83.5^\circ$ $\omega = 2129 \text{ Hz}$
2	 $\theta = 64^\circ$ $\omega = 2413 \text{ Hz}$	 $\theta = 73^\circ$ $\omega = 2096 \text{ Hz}$	 $\theta = 83^\circ$ $\omega = 1775 \text{ Hz}$

Figure 19: Fundamental vibration modes of $[\pm\theta/90/0]_{2s}$ laminated curved panels with four fixed edges and under optimal fiber angles ($b = 10 \text{ cm}$, $\phi = 150^\circ$)

2. The optimal fundamental frequencies of the curved laminated panels with small aspect ratios are greater than those with large aspect ratios. For the curved laminated panels with fixed edges, their optimal fundamental frequencies are greater than those with simply supported edges.
3. When the curved laminated panel has large aspect ratio, small circular angle and subjected to large compressive force, its vibration mode under optimal fiber angle may have more wave numbers in the axial direction.

Acknowledgement: This research work was financially supported by the National Science Council of the Republic of China under Grant NSC 100-2221-E-006-237.

References

- Abaqus, Inc.** (2010): Abaqus Analysis User's Manuals and Example Problems Manuals, Version 6.10. Providence, Rhode Island.
- Abrate, S.** (1994): Optimal Design of Laminated Plates and Shells. *Composite Structures*, Vol. 29, No. 3, pp. 269-286.
- Bert, C. W.** (1991): Literature Review - Research on Dynamic Behavior of Composite and Sandwich Plates - V: Part II. *The Shock and Vibration Digest*, Vol. 23, No. 7, pp. 9-21.
- Chandrashekhara, K.** (1989): Free Vibration of Anisotropic Laminated Doubly Curved Shells. *Computers and Structures*, Vol. 33, No. 2, pp. 435-440.
- Chakrabarti, A.; Topdar, P.; Sheikh, A. H.** (2006): Vibration of Pre-stressed Laminated Sandwich Plates with Interlaminar Imperfections. *Journal of Vibration and Acoustics, ASME*, Vol. 128, No. 6, pp. 673-681.
- Chen, J.-M.** (2009): Optimization of Fundamental Frequencies of Axially Compressed Laminated Curved Panels. M.S. Thesis, Department of Civil Engineering, National Cheng Kung University, Tainan, Taiwan (in Chinese).
- Chen, C.-S.; Cheng, W.-S.; Chien, R.-D.; Doong, J.-L.** (2002): Large Amplitude Vibration of an Initially Stressed Cross Ply Laminated Plates. *Applied Acoustics*, Vol. 63, No. 9, pp. 939-956.
- Chun, L.; Lam, K. Y.** (1995): Dynamic Analysis of Clamped Laminated Curved Panels. *Composite Structures*, Vol. 30, No. 4, pp. 389-398.
- Cook, R. D.; Malkus, D. S.; Plesha, M. E.; Witt, R. J.** (2002): Concepts and Applications of Finite Element Analysis, Fourth Edition. John Wiley & Sons Inc.
- Crawley, E. F.** (1979): The Natural Modes of Graphite/Epoxy Cantilever Plates and Shells. *Journal of Composite Materials*, Vol. 13, No. 3, pp. 195-205.

Dhanaraj, R.; Palanininathan (1990): Free Vibration of Initially Stressed Composite Laminates. *Journal of Sound and Vibration*, Vol. 142, No. 3, pp. 365-378.

Haftka, R. T.; Gürdal, Z.; Kamat, M. P. (1990): Elements of Structural Optimization, Second Revised Edition, Chapter 4. Kluwer Academic Publishers.

Hu, H.-T.; Ho, M.-H. (1996): Influence of Geometry and End Conditions on Optimal Fundamental Natural Frequencies of Symmetrically Laminated Plates. *Journal of Reinforced Plastics and Composites*, Vol. 15, No. 9, pp. 877-893

Hu, H.-T.; Juang, C.-D. (1997): Maximization of the Fundamental Frequencies of Laminated Curved Panels against Fiber Orientation. *Journal of Aircraft*, AIAA, Vol. 34, No. 6, pp. 792-801.

Hu, H.-T.; Ou, S.-C. (2001): Maximization of the Fundamental Frequencies of Laminated Truncated Conical Shells with Respect to Fiber Orientations. *Composite Structures*, Vol. 52, No. 3-4, pp. 265-275.

Hu, H.-T.; Tsai, J.-Y. (1999): Maximization of the Fundamental Frequencies of Laminated Cylindrical Shells with Respect to Fiber Orientations. *Journal of Sound and Vibration*, Vol. 225, No. 4, pp. 723-740.

Hu, H.-T.; Tsai, W.-K. (2009): Maximization of the Fundamental Frequencies of Axially Compressed Laminated Plates against Fiber Orientation. *AIAA Journal*, AIAA, Vol. 27, No. 4, pp. 916-922

Hu, H.-T.; Wang, K.-L. (2007): Vibration Analysis of Rotating Laminated Cylindrical Shells. *AIAA Journal*, Vol. 45, No. 8, pp. 2051-2061.

Narita, Y. (2003): Layerwise Optimization for the Maximum Fundamental Frequency of Laminated Composite Plates. *Journal of Sound and Vibration*, Vol. 263, No. 5, pp. 1005-1016.

Nayak, A. K., Moy, S. S. J., Sheno, R. A. (2005): A Higher Order Finite Element Theory for Buckling and Vibration Analysis of Initially Stressed Composite Sandwich Plates. *Journal of Sound and Vibration*, Vol. 286, No. 4-5, pp. 763-780.

Qatu, M. S.; Leissa, A. W. (1991): Natural Frequencies for Cantilevered Doubly-Curved Laminated Composite Shallow Shells. *Composite Structures*, Vol. 17, No. 3, pp. 227-255.

Raouf, R. A. (1994): Tailoring the Dynamic Characteristics of Composite Panels Using Fiber Orientation. *Composite Structures*, Vol. 29, No. 3, pp. 259-267.

Schmit, L. A. (1981): Structural Synthesis - Its Genesis and Development. *AIAA Journal*, AIAA, Vol. 19, No. 10, pp. 1249-1263.

Sharma, C. B.; Darvizeh, M. (1987): Free Vibration of Specially Orthotropic, Multilayered, Thin Cylindrical Shells with Various End Conditions. *Composite Structures*, Vol. 7, No. 2, pp. 123-138.

Topal, U.; Uzman, U. (2006): Optimal Design of Laminated Composite Plates to Maximize Fundamental Frequency Using MFD Method. *Structural Engineering and Mechanics*, Vol. 24, No. 4, pp. 479-491.

Vanderplaats, G. N. (1984): Numerical Optimization Techniques for Engineering Design with Applications, Chapter 2. McGraw-Hill.

Whitney, J. M. (1973): Shear Correction Factors for Orthotropic Laminates Under Static Load. *Journal of Applied Mechanics*, Vol. 40, No. 1, pp. 302-304.

